Primary Donor Photo-Oxidation in Photosystem I: A Re-Evaluation of ($P700^+$ − P700) Fourier Transform Infrared Difference Spectra[†]

Gary Hastings,*[,‡] V. M. Ramesh,[§] Ruilli Wang,[‡] Velautham Sivakumar,[‡] and Andrew Webber[§]

Department of Physics and Astronomy, Georgia State University, Atlanta, Georgia 30303, and Department of Plant Biology and Center for the Study of Early Events in Photosynthesis, Arizona State University, P.O. Box 871601, Tempe, Arizona 85287-1601

Received July 11, 2001; Revised Manuscript Received September 7, 2001

ABSTRACT: Light-induced Fourier transform infrared (FTIR) difference spectroscopy has been used to study the photo-oxidation of the primary electron donor (P700) in PS I particles from *Chlamydomonas reinhardtii* and *Synechocystis* sp. PCC 6803. To aid in the interpretation of the spectra, PS I particles from a site-directed mutant of *C. reinhardtii*, in which the axial histidine ligand (HisA676) was changed to serine, were also studied. A high-frequency (3300−2600 cm^{-1}) electronic transition is observed for all PS I particles, demonstrating that P700 is dimeric. The electronic band is, however, species-dependent, indicating some differences in the electronic structure of P700 and/or $P700^+$ in *C. reinhardtii* and *Synechocystis* sp. 6803. For PS I particles from *C. reinhardtii*, substitution of HisA676 with serine has little effect on the ester carbonyl modes of the chlorophylls of P700. However, the keto carbonyl modes are considerably altered. Comparison of ($P700^+$ − P700) FTIR difference spectra obtained using PS I particles from the wild type (WT) and the HS(A676) mutant of *C. reinhardtii* indicates that the mutation primarily exerts its influence on the P700 ground state. The 13^1 keto carbonyls of the chlorophylls of P700 of the wild type absorb at similar frequencies, which has previously made these transitions difficult to resolve. However, for the HS(A676) mutant, the 13^1 keto carbonyl of chlorophyll *a* or chlorophyll *a*′ of P700 on PsaB or PsaA absorbs at 1703.4 or 1694.2 cm^{-1}, respectively, allowing their unambiguous resolution. Upon $P700^+$ formation, in both PS I particles from *C. reinhardtii*, the higher-frequency carbonyl band upshifts by ∼14 cm^{-1} while the lower frequency carbonyl downshifts by ∼10 cm^{-1}. The similarity in the spectra for WT PS I particles from *C. reinhardtii* and *Synechocystis* sp. 6803 indicates that a similar interpretation is probably valid for PS I particles from both species. The mutant results allow for an interpretation of the behavior of the 13^1 keto carbonyls of P700 that is different from previous work [Breton, J., Nabedryk, E., and Leibl, W. (1999) *Biochemistry 38*, 11585−11592], in which it was suggested that 13^1 keto carbonyls of P700 absorb at 1697 and 1639 cm^{-1}, and upshift by 21 cm^{-1} upon cation formation. The interpretation of the spectra reported here is more in line with recent results from ENDOR spectroscopy and high-resolution crystallography.

Photosystem I (PS I)[1] is a membrane-bound photosynthetic enzyme that utilizes light to transfer electrons across a membrane from plastocyanin to ferredoxin. In PS I, light absorption ultimately results in the excitation of a specialized chlorophyll (Chl) donor species called P700 (*1*, *2*). The excited state of P700 (P700*) is highly reducing, and an electron is transferred rapidly to a Chl-like acceptor called A_0 (*1*, *2*). The photogenerated radical pair is stabilized by secondary electron transfer (ET) processes; from A_0 the electron is transferred to a phylloquinone acceptor called A_1 (*1*, *2*) and then onto the iron−sulfur cluster F_x, F_A and F_B. In PS I, two sets of ET cofactors are bound to the membrane-spanning protein subunits PsaA and PsaB, and are arranged pseudosymmetrically around a C2 symmetry axis (*3*). At present, it is unclear if one or both branches are involved in ET (*2*, *5*).

In PS I, P700 is a key component in solar conversion as it couples energy transfer processes in the antenna to electron transfer processes in the reaction center. The molecular structural details of P700, the primary donor in PS I, have recently been obtained from X-ray crystallographic studies of PS I particles from *Synechococcus elongatus* at 2.5 Å resolution (*3*). P700 appears to be a dimer of Chl *a* (PsaB side) and Chl *a*′ (PsaA side). Both Chls have axial ligands provided by histidine residues from the PsaA and PsaB protein subunits. The axial ligands to the Chl *a*′ and Chl *a* of P700 are provided by HisA676 and HisB656, respectively, in *Chlamydomonas reinhardtii*. [In *S. elongatus*, the corresponding residues are HisA680 and HisB660. We will use *C. reinhardtii* numbering throughout this manuscript.] The 13^1 keto carbonyl (C═O) of Chl *a*′ on PsaA is hydrogen-bonded to ThrA739. The propionic acid ester C═O of Chl

[†] This work was supported by startup funds, a quality improvement grant, a team grant, and a research initiation grant to G.H. A.W. acknowledges support from the USDA NRICGP.

* To whom correspondence should be addressed. E-mail: phyggh@panther.gsu.edu. Fax: (404) 651-1427. Phone: (404) 651-0748.

[‡] Georgia State University.

[§] Arizona State University.

[1] Abbreviations: C═O, carbonyl; Chl *a*, chlorophyll *a*; DS, difference spectra; ET, electron transfer; FTIR, Fourier transform infrared; PS I, photosystem I; P700, primary electron donor in PS I; PMS, phenazine methosulfate; *S.* 6803, *Synechocystis* sp. PCC 6803.

10.1021/bi0155753 CCC: $20.00
Published on Web 10/03/2001

a′ is H-bonded to TyrA731. In addition, it has been suggested that the 13^3 carbomethoxy ester C═O is H-bonded to water, and that three amino acids (TyrA600, SerA604, and ThrA739) could act as H-bond partners with this water molecule. Interestingly, there are no H-bonds to Chl *a* on PsaB of P700. This H-bonding pattern likely has important implications for the electronic structure of P700, and the directionality of ET in PS I.

Fourier transform infrared (FTIR) difference spectroscopy is sensitive to small structural changes of pigments embedded within proteins. For example, small changes in H-bond strengths or structural alterations of bound water molecules can be detected using this technique (*23*−*25*). In addition, FTIR difference spectroscopy provides molecular specific information about both the resting state and the light-activated state of enzymes (*23*). This type of molecular specific information cannot be gleaned from static crystallographic data. So FTIR difference spectroscopy can strongly complement crystallographic studies, as well as provide a means of experimentally testing crystallographic predictions.

($P700^+$ − P700) FTIR difference spectra (DS) have been obtained by several authors (*4*−*12*). For *C. reinhardtii*, two ($P700^+$ − P700) FTIR DS have been reported using either PS I membranes (*9*) or particles (*12*). The ($P700^+$ − P700) FTIR DS for WT in either of these reports are very different, and in both reports, little insight into the spectra was furnished. It has recently been found that replacement of HisB656 or HisA676 with several different amino acids results in altered optical and physical properties of P700 (*13*). The effects were always more pronounced when HisB656 was replaced, compared to HisA676. In addition, the electron spin density distribution of $P700^+$, determined by ENDOR spectroscopy, was only altered upon replacement of HisB656 (*13*). It was further concluded that the P700 triplet state (^{3}P700) resides on the Chl *a* of P700 on PsaB, the same Chl *a* that carries the bulk of the electron spin density of $P700^+$. This later result is the opposite of conclusions drawn from FTIR studies of P700 (*7*). In addition, FTIR studies of P700 also indicated that the spin distribution over the Chls of $P700^+$ is ∼1:1 to 1:2 (*7*). This also strongly disagrees with ENDOR spectroscopic data, where the spin distribution over the Chls of $P700^+$ is estimated to be ∼1:6 to 1:9 (*13*, *14*). The origin of the discrepancies in the conclusions drawn from the different spectroscopies has never been considered. It is possible that bands in ($P700^+$ − P700) FTIR DS could have been misassigned, which could then result in incorrect conclusions being drawn from the data.

To investigate this possibility, we have used FTIR difference spectroscopy, in combination with site-directed mutagenesis, to study PS I particles from *C. reinhardtii* and *Synechocystis* sp. 6803. We provide evidence that suggests that some of the difference bands in ($P700^+$ − P700) FTIR DS could have been misassigned, and we propose alternative band assignments.

MATERIALS AND METHODS

Detergent-isolated PS I particles from *Synechocystis* sp. 6803 (*S.* 6803) were prepared as described previously (*15*, *16*). The HS(A676) mutant from *C. reinhardtii* was constructed as described previously using a strain that lacks PS II (*13*, *17*). Membrane fragments and purified PS I particles from the HS(A676) mutant were prepared as described previously (*13*).

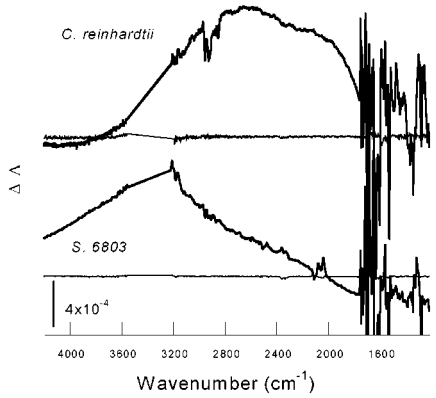

FIGURE 1: ($P700^+$ − P700) FTIR DS in the 4200−1200 cm^{-1} spectral region, obtained using PS I particles from *C. reinhardtii* (top curve) and monomeric PS I particles from *S.* 6803 (bottom curve). A broad, intense water absorbance band is observed near 3400 cm^{-1}, and typical sample absorbance exceeds 1.2 between 3200 and 3570 cm^{-1}. For this reason, we do not present or discuss data in this spectral region. The *C. reinhardtii* spectrum (and the dark − dark spectrum) was scaled by a factor of 3.5 to produce similar bleaching of the 1697−1700 cm^{-1} bands (see Figure 2). The spectra are shifted for ease of comparison and clarity. The thin "flat" lines shown superimposed with each spectrum are dark − dark difference spectra that give a measure of the noise level in each experiment. These spectra have been shifted and do not represent zero absorption. The *C. reinhardtii* spectra were obtained at 2 cm^{-1} resolution, while the *S.* 6803 spectra were obtained at 4 cm^{-1} resolution.

For FTIR experiments, PS I particles from *S.* 6803 or *C. reinhardtii* were pelleted, and placed between a pair of rectangular CaF_2 windows. For some samples, 1 mM ferricyanide and 1 mM ferrocyanide (in D_2O) were added to the pellet. Otherwise, no redox mediators were added. No observable effects of mediator addition were observed in the difference spectra. All experiments described here were performed at room temperature (RT). The absorbance of the sample in the cell was ∼0.7 at the peak of the amide I absorption band. Light minus dark and dark minus dark ($P700^+$ − P700) FTIR difference spectra were recorded as described previously (*5*). The spectral resolution was set at 4 or 2 cm^{-1}.

All spectral curve fitting was performed using the software package OPUS, supplied by Bruker Instruments. Spectra were resolved into combined Lorentzian and Gaussian components by means of a curve-fitting algorithm that utilizes a Levenberg−Marquardt iteration procedure. The "goodness of fit" is quantified by an rms noise parameter. The smaller the rms noise parameter, the better the fit or, more accurately, the closer the fitted curve matches the data. This is important since it is not possible to visually inspect and judge how well the fitted curves match the data.

RESULTS

Figure 1 shows the ($P700^+$ − P700) FTIR DS obtained using PS I particles isolated from *C. reinhardtii* and *S.* 6803, in the 4200−1200 cm^{-1} spectral region. The difference spectra obtained well after (minutes) light excitation are also shown in Figure 1. These spectra give a measure of the noise level in the experiments. For *S.* 6803, a broad band centered near 3300 cm^{-1} is observed. The intensity of the band is

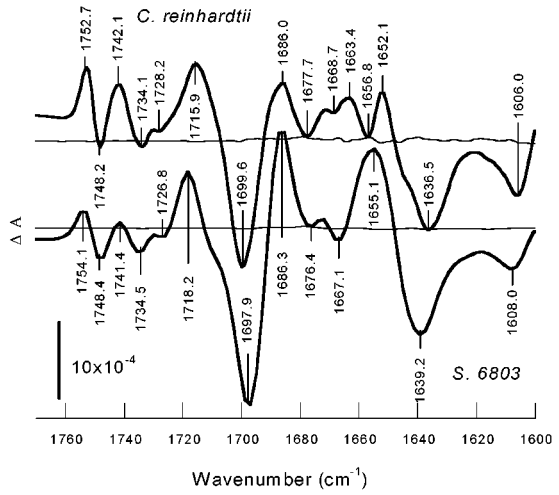

FIGURE 2: (P700$^+$ − P700) FTIR DS from Figure 1, expanded to show the 1770−1600 cm^{-1} spectral region: *C. reinhardtii* (top curve) and *S.* 6803 (bottom curve). The dark − dark difference spectra (noise level) are also taken from Figure 1.

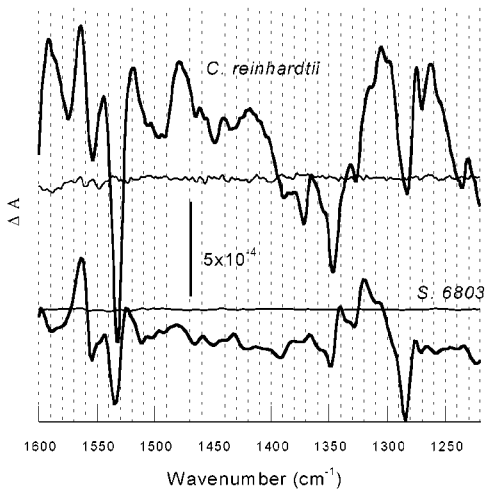

FIGURE 3: (P700$^+$ − P700) FTIR DS from Figure 1, expanded to show the 1600−1220 cm^{-1} spectral region: *C. reinhardtii* (top curve) and *S.* 6803 (bottom curve). The dark − dark difference spectra (noise level) are also taken from Figure 1.

more than twice the intensity of the positive 1754 cm^{-1} band (see Figure 2). For *C. reinhardtii*, a narrower band centered near 2700 cm^{-1}, with a distinct shoulder near 2000 cm^{-1}, is observed. The peak intensity of the ∼2700 cm^{-1} band is similar to that of the positive 1753 cm^{-1} band (see Figure 2).

Figure 2 shows the same spectra as in Figure 1, but in the 1770−1600 cm^{-1} spectral region. The *C. reinhardtii* spectrum was collected at 2 cm^{-1} resolution, as the two difference bands in the 1760−1730 cm^{-1} region were poorly resolved at 4 cm^{-1} resolution (see Figure 4A). This is not the case for the *S.* 6803 spectrum. In the 1760−1600 cm^{-1} region, several difference bands are observed, and overall, the difference spectra are very similar. For *C. reinhardtii* or *S.* 6803, an intense negative band is observed at 1698 or 1700 cm^{-1}, respectively. For *S.* 6803, positive bands are observed at 1686, 1718, 1741, and 1754 cm^{-1}. A distinct shoulder is also observed at 1710 cm^{-1}. In addition, a clear difference band is observed at 1639(−)/1655(+) cm^{-1}. For *C. reinhardtii*, positive bands are observed at 1686, 1716, 1742, and 1753 cm^{-1}. A difference band is also observed at 1637(−)/1652(+) cm^{-1} and displays a shoulder at 1644 cm^{-1}.

Figure 3 shows the same spectra as Figure 1, but in the 1600−1220 cm^{-1} spectral region. For the *C. reinhardtii* spectrum, two intense bands at 1592(+) and 1478(+) cm^{-1} are observed that appear to lack counterparts in the *S.* 6803 spectrum. Other than these two bands, the difference spectra in Figure 3 share many similarities, except that many of the band intensities appear to be greater for the *C. reinhardtii* PS I particles, in particular, the 1533(−) and 1347(−) cm^{-1} bands and the broad, structured positive bands centered near 1305 and 1266 cm^{-1}. The scaling procedure applied to the *C. reinhardtii* spectrum in Figure 3 could lead to a slight overestimation of the amplitude of the bands, but it could not explain such large intensity differences between the spectra. Thus, the band intensities do appear to reflect a real species variation in (P700$^+$ − P700) FTIR difference spectra.

Figure 4 shows (P700$^+$ − P700) FTIR DS for PS I particles from WT and the HS(A676) mutant from *C. reinhardtii* in the 1760−1620 cm^{-1} spectral region. The mutant spectrum has been scaled arbitrarily by a factor of 2. When the spectra are normalized to total protein concentration (by considering the area under the amide I absorption band), it is found that the WT spectrum displays bands that are approximately a factor of 2 more intense than those in the mutant spectrum.

At >1728 cm^{-1}, the spectra for both the WT and the mutant are very similar. However, the negative 1700 cm^{-1} band, observed in the WT spectrum, appears to be split in the HS(A676) mutant spectrum, and two negative peaks at 1703 and 1694 cm^{-1} are observed. This splitting is similar to that observed previously for a PsaA-HQ676 mutant from *C. reinhardtii* (*9*). Furthermore, the 1637(−)/1655(+) cm^{-1} difference band in the WT spectrum appears to be modified in the HS(A676) mutant spectrum, resulting in a 1637(−)/1661(+) cm^{-1} difference band. Finally, the positive 1686 cm^{-1} band in the WT spectrum appears to downshift by 2 cm^{-1} in the HS(A676) mutant spectrum, and its intensity is somewhat decreased.

DISCUSSION

Low-Frequency Electronic Transitions. Both spectra in Figure 1 exhibit broad positive absorption features at >2000 cm^{-1}. For the *C. reinhardtii* spectrum in Figure 1, a clear shoulder is also observed near 1950 cm^{-1}. A broad near-IR band is also observed for the HS(A676) mutant, and its spectrum is identical to the spectrum shown for WT (data not shown). Broad near-IR bands have been observed previously for PS I from *S.* 6803 (*5*, *7*) and *C. reinhardtii* (*12*). In addition, similar broad bands have been observed using PS I from *Acarychloris marina* (*18*), and reaction centers from heliobacteria (*8*, *19*), green sulfur bacteria (*8*, *20*), and purple bacteria (*8*, *21*, *27*). Broad FTIR difference bands at >2000 cm^{-1} are therefore quite characteristic of primary electron donors in photosynthetic organisms and are thought to be due to low-frequency electronic transitions associated with the dimeric nature of the primary electron donor (*21*). Consistent with this is the observation of broad, low-frequency transitions in cation porphyrin dimers, but not in porphyrin monomers (*22*), monomeric Chl *a* in solution (*6*), or heterodimer mutants of purple bacteria in which the oxidized donor is essentially monomeric in character (*27*).

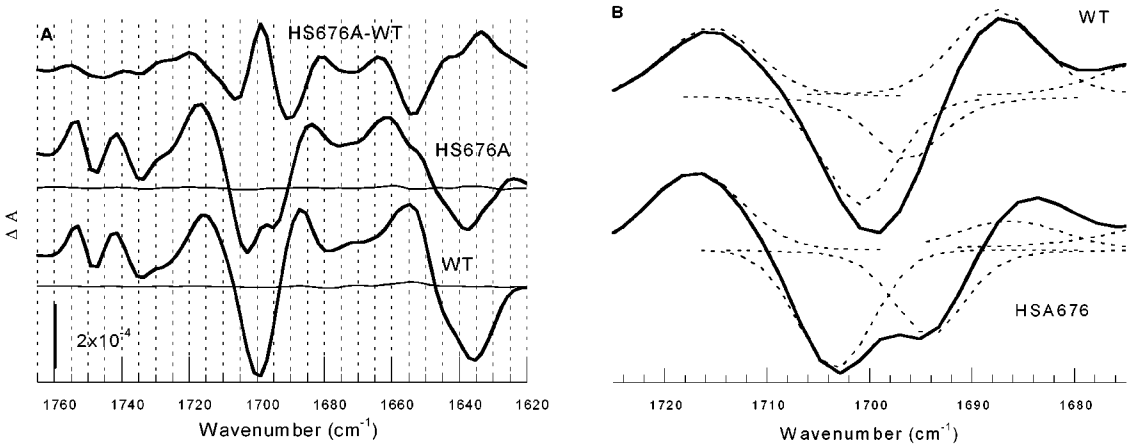

FIGURE 4: (A) ($P700^+ - P700$) FTIR DS in the 1760−1620 cm^{-1} spectral region, obtained using WT PS I particles from *C. reinhardtii* (bottom) and PS I particles of the HS(A676) mutant from *C. reinhardtii* (middle). The difference between the two spectra is also shown (top). Both spectra were obtained at 4 cm^{-1} resolution. (B) Results obtained from nonlinear least-squares curve fitting procedures applied to the two spectra in panel A, in the 1730−1670 cm^{-1} spectral region. The original spectra are shown as solid lines. The spectra were fitted to five components and a baseline. One of the components was used to simulate absorption changes below 1670 cm^{-1}. The four components of interest are shown as dotted lines. The fitted parameters are presented in Table 1. The actual fitted curve is not shown as it is not visibly different from the data.

The broad, positive absorption band(s) observed for *S.* 6803 and *C. reinhardtii* have very different structures, which could indicate that the delocalized charge distribution over the Chls of $P700^+$ is different in *S.* 6803 and *C. reinhardtii*. For *C. reinhardtii*, the broad, positive absorption band displays similarities to the corresponding bands observed in spectra obtained using *Rhodobacter sphaeroides* chromatophores (*21*, *27*) and membranes from the PS I bacterial analogue *Chlorobium limicola* (*8*). This may be an indication that the spin distribution is more delocalized in $P700^+$ from *C. reinhardtii* than in $P700^+$ from *S.* 6803.

A variety of magnetic spectroscopies have been used to estimate the degree of delocalization of the charge over the chls of $P700^+$ (see ref *14* for a review), and ratios of 3:1 up to 9:1 have been obtained (*14*). Given the large variation of the ratios, it has not been possible to distinguish differences in $P700^+$ from algal or cyanobacterial preparations using magnetic spectroscopic techniques.

Dimer "Marker Modes". In FTIR DS associated with donor oxidation in *Rb. sphaeroides*, positive FTIR difference bands with high intensity are observed at ∼1550, 1480, and 1295 cm^{-1} (*8*). These bands have been related to the dimeric nature of the primary donor and are good marker bands for multimeric pigment species (*8*, *21*). Similar, high-intensity, IR bands are observed for heliobacterial (*8*, *19*) and green sulfur bacterial (*8*, *20*) reaction centers. For *C. reinhardtii*, it has been suggested that the relatively intense, broad, structured bands near 1305 and 1270 cm^{-1} in Figure 3 could correspond to similar dimeric marker bands (*12*). It could also be possible that the broad, structured positive peak centered near 1320 cm^{-1} in the *S.* 6803 spectrum has the same origin as the 1305 and 1270 cm^{-1} bands in the *C. reinhardtii* spectrum.

WT FTIR Difference Spectra. Overall, the ($P700^+ - P700$) FTIR DS for *C. reinhardtii* (WT) and *S.* 6803 are very similar in the 1760−1600 cm^{-1} spectral region (Figure 2). This indicates that it is likely that any interpretation of the difference bands in terms of detailed bonding interactions is probably valid for the spectra from both species. The ($P700^+ - P700$) FTIR difference spectrum for *C. reinhardtii* (WT) is similar to that reported by Leibl et al. (*12*) but is very different from the spectrum reported by Redding et al. (*10*). PS I particles or membranes from different strains of *C. reinhardtii* were used in the two studies; however, it is unlikely that this would account for the differences in the spectra, given the overall similarity that we observe for spectra from different species in Figure 2.

For the spectra in Figure 2, the intensity of the ∼1700 cm^{-1} band is approximately the same. For the *C. reinhardtii* spectrum in Figure 3, a scaling identical to that in Figure 2 was used. Both spectra in Figure 3 display a similar band pattern; however, many of the bands in the *C. reinhardtii* spectrum appear to be significantly increased in intensity, compared to that in the *S.* 6803 spectrum. The 1564(+)/1554(−) cm^{-1} difference band is thought to be associated with amide II absorption and appears to be similar in intensity for both species (*7*). The 1533−1537 cm^{-1} negative band is significantly increased in intensity in the *C. reinhardtii* spectrum. This band is thought to be associated with the coupled C−C, C−H, and C−N modes of the Chl macrocycle (*7*, *26*), as are the 1283−1285 and 1347−1349 cm^{-1} bands in both spectra in Figure 3 (*7*, *26*). Consistent with this is the fact that similar negative bands at the same frequencies are also observed in electrochemically generated $Chl^+ - Chl$ FTIR DS (*6*). At present, we do not have a satisfying explanation for the observation of higher-intensity bands in the 1600−1200 cm^{-1} region, in ($P700^+ - P700$) FTIR DS obtained using PS I particles from *C. reinhardtii*. One possibility is that the charge on $P700^+$ is more delocalized over the Chls of P700 in *C. reinhardtii* than in *S.* 6803. This hypothesis would indicate increased contributions from Chl macrocycle modes to the difference spectra for *C. reinhardtii*, compared to those for *S.* 6803. This hypothesis could also explain why the near-IR electronic transition observed for *C. reinhardtii* (Figure 1) is significantly different from that observed for *S.* 6803.

The 13^3 Ester C═O Stretch Region. The C═O groups of the Chls of P700 absorb in the 1760−1630 cm^{-1} spectral region. For P700, there are six C═O groups. Some of the C═O modes have been assigned upon comparison to FTIR

spectra of monomeric Chl *a* and its cation in organic solvent (*6*). For *S.* 6803, the 1748(−)/1754(+) and 1735(−)/1741(+) cm^{-1} difference bands were assigned to an upshift of the 13^3 ester C═O groups of the Chls of P700 upon cation formation (*6*, *7*, *10*). The higher-frequency ester C═O mode is most likely to be free of H-bonding. So, when recent crystallographic data are taken into account (*3*), this would indicate that the 1748(−)/1754(+) cm^{-1} difference band is due to the 13^3 ester C═O group of Chl *a* on PsaB, while the 1735(−)/1741(+) cm^{-1} band is due to the 13^3 ester C═O group of Chl *a*' on PsaA, which is H-bonded, via a water molecule, to TyrA600, SerA604, or/and ThrA739. The 1741(+)/1735(−) cm^{-1} band was observed to downshift by ∼6 cm^{-1} upon uniform ^2H labeling (*7*). It was suggested that this shift could be due to deuteration of the methyl hydrogens at the 13^4 position of ring V of Chl *a*′. However, it was later found that the 1735(−)/1741(+) cm^{-1} band downshifts by 2 cm^{-1} upon 13^4 methyl deuteration (*10*). The differences are almost certainly related to the complex H-bonding of the 13^3 ester C═O group of Chl *a*′. Upon 13^4 methyl deuteration of the Chls of P700, several further bands throughout the 1760−1660 cm^{-1} region were also observed to shift (*10*). From this observation, it was suggested that the ester C═O groups of the Chls of P700 are heterogeneously distributed in frequency, which results from local heterogeneity in the protein environment (*10*). A more plausible explanation for multiple band shifts observed upon 13^4 methyl deuteration of the Chls of P700 is that the multiple bands reflect perturbations of protein and water modes that are coupled to the 13^3 ester C═O group of Chl *a*′.

In Figure 4A, it appears that many of the features in the $(P700^+ - P700)$ FTIR DS are shared between WT PS I particles and the HS(A676) mutant of *C. reinhardtii*. This would indicate that the effect of substituting His with Ser at A676 is quite localized and does not cause significant alteration of the protein backbone. The ester C═O modes appear to be unaffected by substituting HisA676 for serine (Figure 4A), although the keto C═O modes do appear to be modified. Below we will discuss the nature of the keto C═O modes of P700, concentrating on *C. reinhardtii*. Given the similarity in the spectra in Figure 2, it is likely that the keto C═O modes of P700 in *S.* 6803 can be described similarly.

The 13^1 Keto C═O Stretch Region. The negative band at 1697−1700 cm^{-1} in both spectra in Figure 2 is thought to be due to the 13^1 keto C═O group of one (*7*) or both (*11*) of the Chl molecules of P700. Breton et al. (*7*) suggest that the 1697 cm^{-1} band is due to a single Chl *a* 13^1 keto C═O mode that upshifts to 1718 cm^{-1} upon cation formation, as it does in Chl *a* (*6*). The 13^1 keto C═O group of the other Chl of P700 was suggested to absorb at 1639 cm^{-1}, which upshifts to 1658 cm^{-1} upon cation formation (*7*; see Figure 2). Such a low-frequency keto C═O mode could indicate that the C═O group is strongly H-bonded. In view of recent crystallographic data (*3*), this would indicate that the 1639 cm^{-1} band is due to the keto C═O mode of Chl *a*′, which is H-bonded to ThrA739. The assignment of the 1639(−)/1658(+) cm^{-1} difference band to a keto C═O mode of one of the Chls of P700 was based upon the observation of a single intense negative band at 1639 cm^{-1} in $(^3P700 - P700)$ FTIR DS, and the fact that the triplet state is thought to reside on a single Chl of P700 (*7*). The observation of a band at 1639 cm^{-1} in $(^3P700 - P700)$ FTIR DS necessarily implies that the triplet state must be localized on Chl *a*′ of P700 on PsaA. This conclusion is the opposite of conclusions drawn from magnetic spectroscopies, which provided clear evidence that the triplet state of P700 is localized on the PsaB Chl *a* of P700 (*13*, *14*).

Given the interpretation of FTIR DS postulated by Breton et al. (*7*) and the fact that both keto C═O modes upshift by the same amount upon cation formation, it was further suggested that the charge on $P700^+$ exhibited appreciable delocalization over both Chls of P700. The ratio of charge delocalization was estimated to be ∼1:1 to 2:1. This ratio also strongly disagrees with conclusions drawn from ENDOR spectroscopy, where a ratio of 6:1 to 9:1 was calculated, indicating appreciable charge localization on PsaB Chl *a* of P700 (*13, 14*).

Hamacher et al. (*11*) outlined an alternative interpretation for the $(P700^+ - P700)$ FTIR DS that was, admittedly, not based on experimental data. They suggested that both 13^1 keto C═O groups of both Chls of P700 contributed to the 1697−1700 cm^{-1} band and that one C═O group upshifts to 1718 cm^{-1} while the other downshifts to 1686 cm^{-1} upon cation formation. This hypothesis provides an explanation for the positive 1686 cm^{-1} band. In addition, this hypothesis could help resolve the discrepancies between FTIR and EPR data, as it suggests quite an asymmetry in the charge distribution over the Chls of P700.

When the above hypothesis is considered and the PS I crystallographic data are taken into account (*3*), as well as the fact that the 13^1 keto C═O mode of Chl *a* in solution upshifts upon cation formation, the 1697−1700 cm^{-1} mode that upshifts to 1718 cm^{-1} is likely due to the 13^1 keto C═O mode of Chl *a* on PsaB. The 1697−1700 cm^{-1} mode that downshifts is then due to the 13^1 keto C═O mode of Chl *a*′ on PsaA, which is H-bonded to ThrA739. This hypothesis could indicate that much of the charge on $P700^+$ is located on PsaB (as this mode upshifts upon cation formation), in agreement with magnetic spectroscopic data. Furthermore, given the above hypothesis, the similarity in the frequency of the C═O modes in the ground state indicates that ThrA739 provides a relatively weak H-bond.

Substituting HisA676 results in a splitting of the 1700 cm^{-1} band without other gross alterations in the spectra (Figure 4A). This fact alone indicates that more than one species contributes to the 1700 cm^{-1} band in WT PS I particles from *C. reinhardtii*. The splitting of the 1700 cm^{-1} band makes the 1730−1670 cm^{-1} region of the spectrum amenable to accurate and unambiguous curve fitting analysis (Figure 4B and Table 1).

For the HS(A676) mutant, the split negative band is best described by two negative bands at 1694.2 and 1703.4 cm^{-1} with widths of 8 and 8.5 cm^{-1}, respectively. It is likely that the higher-frequency band is due to the keto C═O mode of Chl *a* on PsaB, because it is free from H-bonding. From Table 1, the 1703.4 cm^{-1} band upshifts to 1717.0 cm^{-1} while the 1694.2 band downshifts to ∼1684.5 cm^{-1} upon cation formation. Notice that the curve fit parameters outlined in Table 1 for the HS(A676) mutant are close to unique. Only very small but negligible variations in the parameters yield optimal fits, as judged by a minimized χ^2 parameter. Notice that the 1684.5 cm^{-1} band, for the HS(A676) mutant, is reduced in intensity relative to the 1687.3 cm^{-1} band in the

Table 1: Results Obtained from Nonlinear Least-Squares Curve Fitting Procedures Applied to the Two Spectra in Figure 4A, in the 1730−1670 cm^{-1} Spectral Region[a]

C. reinhardtii	band center	bandwidth	assignment
WT	1687.3 (+)	8.6	$C{=}O_A^+$
	1697.4 (−)	7.8	$C{=}O_A$
	1701.7 (−)	9.2	$C{=}O_B$
	1715.6 (+)	13.5	$C{=}O_B^+$
HS(A676)	1684.5 (+)	10.3	$C{=}O_A^+$
	1694.2 (−)	8.0	$C{=}O_A$
	1703.4 (−)	8.5	$C{=}O_B$
	1717.0 (+)	10.8	$C{=}O_B^+$

[a] All results are in inverse centimeters. The assignments refer to the 13^1 keto C═O groups of the Chls of P700 on PsaA or PsaB (subscripts) in either the ground or excited state.

WT spectrum. This is probably due to complex overlap with bands at <1680 cm^{-1}.

Using the curve fitting parameters for the HS(A676) mutant as starting parameters, we also fitted the WT spectra. The optimized parameters that resulted are presented in Table 1. When the parameters in Table 1 are compared, it appears that the negative 1700 cm^{-1} band in the WT spectrum can be deconvolved into two bands that absorb at 1697.4 and 1701.7 cm^{-1}. Upon substitution of HisA676 with serine, the 1697.4 cm^{-1} band downshifts to 1694.2 cm^{-1} while the 1701.7 cm^{-1} band upshifts to 1703.4 cm^{-1}. Thus, the mutation has a much larger effect on the C═O mode of Chl *a*′ on PsaA, as is expected. Importantly, substitution of HisA676 with serine perturbs the structure of P700 in the ground state. This indicates that any analysis of mutant-induced modifications of the $P700/P700^+$ midpoint potential should consider changes in the energy levels of both P700 and $P700^+$.

For WT PS I particles from *C. reinhardtii*, the 1697.4 and 1701.7 cm^{-1} bands downshift and upshift by 10.1 and 13.9 cm^{-1}, respectively, upon cation formation. Almost identical shifts are observed for PS I particles from the HS(A676) mutant, where the 1694.2 and 1703.4 cm^{-1} bands downshift and upshift by 10.3 and 13.6 cm^{-1}, respectively, upon cation formation. This observation suggests that substitution of HisA676 with serine does not alter the charge distribution over the Chls of $P700^+$.

Krabben et al. (*13*) observed that the ENDOR properties of $P700^+$ in the HS(A676) mutant were identical to that of WT. So, at least in this case, FTIR DS offer a more suitable molecular specific probe than ENDOR spectroscopy. ENDOR spectroscopy specifically probes structural changes associated with $P700^+$. Since the FTIR data suggest that HisA676 substitution predominantly affects the ground state of P700, it may not be surprising that ENDOR spectroscopy could not detect alterations induced by mutation of HisA676.

If the 1694−1697 cm^{-1} band (Table 1) is assigned to the 13^1 keto C═O mode of Chl *a*′ on PsaA, which is H-bonded to ThrA739, then the fact that the 1694−1697 cm^{-1} band downshifts would indicate a strengthening of the H-bond upon cation formation. The strengthening of the H-bond is probably more pronounced than would be indicated by a 10 cm^{-1} downshift, since positive charge on Chl *a*′ would cause an upshift of the keto C═O mode (*6*). A strengthening of the H-bond could arise from structural modifications that decrease the length of the H-bond.

Given the appropriateness of our interpretation, the question of the origin of the 1637−1639(−)/1652−1655(+) cm^{-1} difference band arises (see Figures 2 and 4A, WT spectra). For the *C. reinhardtii* spectrum in Figure 2, the shape of the ∼1637 cm^{-1} band indicates that it contains contributions from at least two overlapping bands. This is less obvious for the *S.* 6803 spectrum in Figure 2. The ∼1637 cm^{-1} band observed for WT *C. reinhardtii* in Figure 4A is reduced in intensity and shifted upon substitution of HisA676 with serine. This is a further indication that the negative 1636 cm^{-1} band in the WT spectrum in Figure 4A consists of at least two contributions. The HS676 − WT double difference spectrum in Figure 4A displays a differential signal at ∼1634(+) or 1654(−) cm^{-1}, which indicates the complete loss of a ∼1634(−) or 1654(+) cm^{-1} difference band in the WT spectrum, respectively, upon substitution of His(A676) with serine. The most obvious interpretation of these observations is that the ∼1634(+)/1654(−) cm^{-1} band in the double difference spectrum is associated with a vibrational mode of HisA676. Singly protonated histidine in vitro generally displays bands below 1600 cm^{-1} (*28*). However, from FTIR studies (*28*−*29*) and density functional theory calculations (*29*), it was found that the imidazolium cation (doubly protonated 4-methylimidazole) displays a very strong absorption band at 1633 cm^{-1}, which is due predominantly to the $C_4{=}C_5$ stretching vibration of the imidazole ring (*29*). It may be that a singly protonated histidine, with its free nitrogen involved in axial ligation, is a reasonable approximation (in terms of its $C_4{=}C_5$ stretching vibration) to an imidazolium cation. Calculations based on the three-dimensional crystal structure will be required to determine if a protonated histidine residue that is ligated to Chl *a*' could give rise to imidazole vibrational modes at frequencies as high as 1637 cm^{-1}. If the 1637 cm^{-1} band in Figure 4A (WT spectrum) is due to an imidazole mode, then the ∼20 cm^{-1} upshift observed upon cation formation could indicate a decrease in the length of the imidazole $C_4{=}C_5$ bond of ∼0.002 Å (*29*). Furthermore, the above interpretation could indicate that a vibrational mode of HisB656 also contributes to the 1637 cm^{-1} band in the WT spectrum. This mode is not shifted upon substitution of HisA676, so the 1638(−)/1662(+) cm^{-1} difference band in the HS(A676) spectrum in Figure 4A would be due to HisB656. We will use isotopically labeled HS(A676) and HS(B656) site-directed mutants to test this idea.

Conclusion. Our data indicate that the negative 1697−1700 cm^{-1} band, observed in spectra from both species, is due to 13^1 keto C═O modes of both Chls of P700. This conclusion is based upon the observation of a splitting of the 1700 cm^{-1} band into two components upon substitution of HisA676 with serine, and the fact that no other clear alterations to the spectra were observed. Our interpretation of ($P700^+$ − P700) FTIR DS is more consistent with recent results from ENDOR spectroscopy (*13*, *14*) and high-resolution crystallography (*3*), both of which indicate pronounced asymmetry in the primary donor.

ACKNOWLEDGMENT

Whole cells of *S.* 6803 were a gift from Prof. Wim Vermass at Arizona State University.

REFERENCES

1. Golbeck, J. H., and Bryant, D. A. (1991) *Curr. Top. Bioenerg. 16*, 83−175.
2. Brettel, K. (1997) *Biochim. Biophys. Acta 1318*, 322−373.
3. Jordan, P., Fromme, P., Witt, H., Klukas, O., Saenger, W., and Krauss, N. (2001) *Nature 411*, 909−917.
4. Hastings, G. (2001) *Appl. Spectrosc. 55*, 894−900.
5. Hastings, G., and Sivakumar, V. (2001) *Biochemistry 40*, 3681−3689.
6. Nabedryk, E., Leonhard, M., Mäntele, W., and Breton, J. (1990) *Biochemistry 29*, 3242−3247.
7. Breton, J., Nabedryk, E., and Leibl, W. (1999) *Biochemistry 38*, 11585−11592.
8. Nabedryk, E., Leibl, W., and Breton, J. (1996) *Photosynth. Res. 48*, 301−308.
9. Redding, K., MacMillan, F., Leibl, W., Brettel, K., Hanley, J., Rutherford, A. W., Breton, J., and Rochaix, J. D. (1998) *EMBO J. 17*, 1, 50−60.
10. Kim, S., and Barry, B. (2000) *J. Am. Chem. Soc. 122*, 4980−4981.
11. Hamacher, E., Kruip, J., Rogner, M., and Mäntele, W. (1996) *Spectrochim. Acta A52*, 107−121.
12. Leibl, W., Brettel, K., Nabedryk, E., Breton, J., Rochaix, J., and Redding, K. (1998) in *Photosynthesis: Mechanisms and Effects* (Garab, G., Ed.) Vol. I, pp 595−598.
13. Krabben, L., Schlodder, E., Jordan, R., Carbonera, D., Giacometti, G., Lee, H., Webber, A., and Lubitz, W. (2000) *Biochemistry 39*, 13012−13025.
14. Webber, A., and Lubitz, W. (2001) *Biochim. Biophys. Acta* (in press).
15. Hastings, G., Reed, L., Lin, S., and Blankenship, R. E. (1995) *Biophys. J. 69*, 2044−2055.
16. Hastings, G., Hoshina, S., Webber, A., and Blankenship, R. E. (1995) *Biochemistry 34*, 15512−15522.
17. Lee, H., Bingham, S., and Webber, A. (1998) *Methods Enzymol. 297*, 310−320.
18. Hastings, G., Wang, R., and Sivakumar, V. (2001) *Biochim. Biophys. Acta* (submitted for publication).
19. Noguchi, T., Fukami, Y., Oh-oka, H., and Inoue, Y. (1997) *Biochemistry 36*, 12329−12336.
20. Noguchi, T., Kusumoto, N., Inoue, Y., and Sakurai, H. (1996) *Biochemistry 35*, 15428−15435.
21. Breton, J., Nabedryk, E., and Parson, W. (1992) *Biochemistry 31*, 7503−7510.
22. Binstead, R., and Hush, N. (1993) *J. Phys. Chem. 97*, 13172−13179.
23. Mantele, W. (1993) *Trends Biochem. Sci. 18*, 197−202.
24. Nabedryk, E. (1996) in *Infrared Spectroscopy of Biomolecules* (Mantsch, H., and Chapmann, D., Eds.) pp 39−81, Wiley-Liss, Inc., New York.
25. Mäntele, W. (1993) in *The Photosynthetic Reaction Center* (Deisenhoffer, J., and Norris, J., Eds.) Vol. II, p 239, Academic Press, San Diego.
26. Lutz, M., and Mantele, W. (1991) in *Chlorophylls* (Scheer, H., Ed.) 2nd ed., p 855, CRC Press, London.
27. Nabedryk, E., Schulz, C., Muh, F., Lubitz, W., and Breton, J. (2000) *Photochem. Photobiol. 71*, 582−588.
28. Berthomieu, C., and Boussac, A. (1995) *Biospectroscopy 1*, 187−206.
29. Hasegawa, K., Ono, T., and Noguchi, T. (2000) *J. Phys. Chem. B 104*, 4253−4265.

BI0155753